OXFORD UNIVERSITY PRESS | Plant and Cell Physiology

The Di2/pet variant in PETALOSA gene underlies a major heat requirement-related QTL for blooming date in peach (P. persica L. Batsch)

Journal:	*Plant and Cell Physiology*
Manuscript ID	PCP-2020-E-00368
Manuscript Type:	Regular Paper
Date Submitted by the Author:	07-Sep-2020
Complete List of Authors:	Cirilli, Marco; University of Milan, Department of Agricultural Science (DISAA); Dipartimento DISAA Gattolin, Stefano; IBBA CNR, Istituto di Biologia e Biotecnologia Agraria Chiozzotto, Remo; University of Milan, Department of Agricultural Science (DISAA) Baccichet, Irina; University of Milan, Department of Agricultural Science (DISAA) Quilot-Turion, Benedicte; INRAE, Unit Genetics and Breeding of Fruit and Vegetables Pascal, Thierry; INRAE, Unit Genetics and Breeding of Fruit and Vegetables Rossini, Laura; University of Milan, Department of Agricultural Science (DISAA) Bassi, Daniele; University of Milan, Department of Agricultural Science (DISAA)
Keywords:	Flowering, QTL mapping, gene, phenology

Cover

Title: The *Di2/pet variant in* PETALOSA gene underlies a major heat requirement-related QTL for blooming date in peach (*P. persica* L. Batsch)

Running Title: Characterization of major QTL for blooming date in peach

Corresponding author

D. Bassi, Università degli Studi di Milano – DiSAA, Milano, Italy, e-mail: daniele.bassi@unimi.it

L. Rossini, [1]Università degli Studi di Milano – DiSAA, Milano, Italy, e-mail: laura.rossini@unimi.it

Subject areas: (2) environmental and stress responses, (10) genomics, systems biology and evolution

The manuscript includes: 5 colour figures and 1 Table; 5 Supplemental Figures, 2 Supplemental Tables and 1 Supplemental File as Supplementary material.

This article has been accepted for publication in Plant and Cell Physiology Published by Oxford University Press
https://academic.oup.com/pcp/advance-article/doi/10.1093/pcp/pcaa166/6064162?login=true

Main Title

The *Di2/pet variant in* PETALOSA gene underlies a major heat requirement-related QTL for blooming date in peach (*P. persica* L. Batsch)

Running Title

Characterization of major QTL for blooming date in peach

Authors list

Marco Cirilli[1], Stefano Gattolin[2], Remo Chiozzotto[1], Irina Baccichet[1], Thierry Pascal[3], Bénédicte Quilot-Turion[3], Laura Rossini[1], Daniele Bassi[1]

Affiliations

[1]Università degli Studi di Milano – DiSAA, Milano, Italy

[2]CNR-Consiglio Nazionale delle Ricerche, Istituto di Biologia e Biotecnologia Agraria (IBBA), Milano, Italy

[3]INRAE, GAFL, F-84143 Montfavet, France

Corresponding author

Daniele Bassi, e-mail: daniele.bassi@unimi.it

Laura Rossini, e-mail: laura.rossini@unimi.it

Keywords

Flowering, QTL mapping, gene, phenology

Abstract

Environmental adaptation of deciduous fruit trees largely depends on their ability to synchronize growth and development with climate seasonal change. Winter dormancy of flower buds is a key process to prevent frost damage and ensure reproductive success. Temperature is a crucial environmental stimulus largely influencing the timing of flowering, only occurring after fulfillment of certain temperature requirements. Nevertheless, genetic variation affecting chilling or heat-dependent dormancy release still remains largely unknown. In this study, a major QTL able to delay blooming date in peach by increasing heat-requirement was finely mapped in three segregating progenies, revealing a strict association with a genetic variant (pet_{DEL}) in a PETALOSA gene, previously shown to also affect flower morphology. Analysis of segregating genome-edited tobacco plants provided further evidence of the potential ability of PET-

variations to delay flowering time. Potential applications of the ***pet***$_{DEL}$ variant for improving phenological traits in peach are discussed.

Introduction

As a sessile organism, plants require an accurate and continuous monitoring of environmental conditions to ensure the reproductive success and tree survival. An intricate genetic and epigenetic network integrates environmental and endogenous cues, and fine-tunes the proper timing of vegetative to flowering transition (Horvath et al., 2003; Fadón et al., 2015). In model annual species such as Arabidopsis and rice (Dennis and Peacock, 2007; Andres and Coupland, 2012), floral integrator genes, such as *FLOWERING LOCUS T* (*FT*), *SUPPRESSOR OF OVEREXPRESSION OF CONSTANS* (*SOC1*), *TERMINAL FLOWER 1* (*TFL1*), integrate signals from photoperiod, vernalization, autonomous pathways, hormones and aging (Srikanth and Schmid, 2011). They converge on the expression of meristem identity genes such as LEAFY (LFY) and APETALA1 (AP1), in turn directing floral organ patterning by activating homeotic genes of the MADS and AP2 families (Krizek and Fletcher, 2005). Among the environmental stimuli, temperature crucially contributes to the timing of floral transition. Vernalization is a rather well-characterized process of flower induction by prolonged cold exposure mediated by the pivotal gene *FLOWERING LOCUS C (FLC)* (Michaels and Amasino, 1999). A more general role of ambient temperature (e.g. the physiological, non-stressful temperature range of a given species) is also beginning to be clarified. For example, relative abundance of alternative splicing variants of the gene *FLOWERING LOCUS M (FLM)* controls flowering time in response to changes in ambient temperature in Arabidopsis (Posé et al., 2013). In perennial species, the control of flowering is more complex although the function of some floral genes seems to be conserved compared to annual plants. In temperate deciduous trees, flower initiation often occurs autonomously (e.g. mostly regulated by internal cues) while flower organ growth and blooming only occurs the following year, after certain temperature requirements have been fulfilled (Lang et al., 1987).

Peach [*Prunus persica* (L.) Batsch] is a model species for horticultural trees and an excellent system for studying environmental regulation of phenology, which largely controls the onset of developmental processes essential for flower and fruit production (Guo et al., 2014). In peach, floral induction seems to occur early in the season (late spring), although morphological changes associated with the reproductive transition (e.g. the broadening and thickening of the dome apex) only become evident between the end of summer and the beginning of autumn, depending on cultivar and growing environment (Warriner et al., 1985). Flower organogenesis

progresses until the complete differentiation of floral whorls in late autumn (Engin et al., 2007), when trees enter in endo-dormancy, a state of physiological inhibition of flowering induced by cold temperatures and/or short photoperiods (Lang et al., 1987). After the exposure to a certain period of low temperatures, buds re-acquire the competency to respond to external stimuli, passing to an eco-dormant state, until suitable conditions allow growth resumption and budburst (Reinoso et al., 2002). In *Prunus*, specific metabolic and transcriptional patterns seem to distinctly mark endo-dormancy establishment, eco-dormancy transition and blooming onset, suggesting the lack of a 'true' resting state and, rather, a continuous process of organogenesis (Chmielewski et al., 2017; Fadón et al., 2018; Zhang et al., 2018; Yu et al., 2020). In the absence of morphological, biochemical and/or physiological markers, temperature-based models (e.g. chilling, CR, and heat requirements, HR) have been developed (and are widely used) for monitoring dormancy-associated events and accounting for the significant influence of the environment (Weinberger, 1950; Richardson et al., 1974; Fishman et al., 1987; Luedeling, 2011). However, the accuracy of thermal models to predict blooming time is affected by genotype, and both seasonal and local effects, resulting in a variable interaction among CR, HR and Blooming date (BD). In peach, CR seems to have a much stronger effect compared to HR, being closely related with BD and a major source of variability, at least in warmer climates (Fan et al., 2010). In contrast, the contribution of HR remains elusive and is primarily considered a result of excessive chilling (Couvillon and Erez, 1985; Okie et al., 2011). QTLs associated to BD have been mapped in peach (Quilot et al., 2004; Fan et al., 2010; Romeu et al., 2014; Zhebentyayeva et al., 2014) and other stone fruits including almond (Sánchez-Pérez et al. 2012), apricot (Olukolu et al., 2009) and sweet cherry (Castède et al., 2015). Comparative genomic analyses showed that QTL intervals are largely collinear among the different stone fruits (Dirlewanger et al. 2012), suggesting that gene networks underlining flowering control are likely conserved across Prunoideae. Nevertheless, molecular evidence as well as the genetic determinants of BD still remain largely unknown, particularly those related to seasonal fluctuation of environmental temperature. A notable exception has been the characterization of a non-dormant peach mutant ('Evergrowing', EVG), leading to the identification of a MADS-box gene cluster involved in apical shoot growth arrest and dormancy (Bielenberg et al. 2004; Li et al., 2009). The availability of a peach reference genome sequence has allowed the identification of the homologous gene families discovered in model species (Wells et al., 2015). Although the functionality of proteins appears largely conserved (Zhang et al., 2015), their biological role in flowering networks has not yet been elucidated in peach, nor has their link with genetic and phenotypic variability been associated to the response to environmental conditions.

In this work, a genome-wide association study (GWAS) was conducted to dissect BD in a peach collection located in a northern Italy environment. Among the identified loci, a major QTL for BD (named qBD6.1), was finely mapped in three segregating progenies, revealing a strict association with a genetic variant (pet_{DEL}) in a PETALOSA gene, previously shown to affect flower morphology. Analysis of PET-edited tobacco plants provided further evidence of the potential ability of this variant to delay blooming in peach by affecting HR fulfillment.

Results

Association mapping for blooming date in a peach collection

Blooming date (BD) was recorded in a germplasm collection of 133 accessions in two consecutive years in Imola, Northern Italy. BD showed a similar range of variation when comparing the two seasons, 80 – 90 and 97 – 108 Julian Days (JD) respectively in 2012 and 2013 (**Figure 1A**). Although flowering started about 20 days later in 2013, the relative order of genotypes' BDs was significantly correlated across the two seasons (r-squared 0.86, *p*-value < 0.05). The double flower accession 'NJ Weeping' was the latest accession to bloom in both years. After adjusting for kinship and population structure (K = 3), GWAS detected significant marker-trait associations above the Bonferroni threshold ($9.15e^{-06}$) on chromosomes (chr.) 8 (in both years), 4 and 6 (only BD2013). Signals on chr. 4 and 6 were also present in BD2012, although above the less stringent permutation threshold (*p*-value of $2.05e^{-03}$) (**Figure 1B**). Minor signals were also found on chr. 1, 2 and 3 (only BD2012) and 5 (only BD2013). As deduced by QQ-plot inspection, the *p*-values distribution suggests a low number of false positive associations (**Figure 1C**) while heritability was similar in both datasets (0.44 and 0.53). Analysis of linkage disequilibrium (LD) surrounding loci on chr. 4, 6 and 8 reveals high LD levels (> 0.70) between SNPs peaks and the presence of extended LD blocks. Markers SNP_IGA_386778 and SNP_IGA_381543, located at the beginning of chr. 4, explained the highest percentage of phenotypic variance, with an r-squared of 0.20 and 0.26, respectively in 2012 and 2013. Statistical information on associated SNPs is summarized in **Table 1**.

Linkage mapping in a segregating progeny for blooming date

Among the identified markers, SNP_IGA_682343 and SNP_IGA_682704 map to a local LD block on chr. 6 (named q*BD6.1*) spanning about 3.0 Mbp between 22,978,897 - 26,225,619 Mb (delimited by SNP678060 and SNP688290). This genomic region also encompasses the *Di2* locus controlling the dominantly inherited double flower (DF) trait (**Supplemental Figure 1**) (Gattolin et al., 2018). The presence of some DF accessions in the GWAS panel raises the hypothesis of the possible involvement of the *Di2* locus in blooming time. To further investigate

the linkage between BD and DF traits, we analyzed an F2 progeny (WFPxP) derived from the cross 'Weeping Flower Peach' (a DF accession) x 'Pamirskij 5' (single flower, SF). This population segregates for the three genotypes at *Di2* locus (*di2/di2*, single, *Di2/di2* and *Di2/Di2* double flower), although with a deviation of the expected inheritance pattern, with an excess of single-flower seedlings (Pascal et al., 2017). WFPxP showed a wide quantitative variability for BD, ranging from 76 to 100 JD with a negatively skew distribution towards late blooming genotypes (**Figure 2A**). QTL analysis revealed the presence of a major BD locus on chr. 6 (**Figure 2B**), while no additional loci were detected in other genomic regions (**Supplemental Figure 2**). The 2-LOD confidence interval (CI) delimits this major QTL to a physical region of about 0.5 Mb (23,906,028 - 24,402,489) between SNP680310 and SNP681888. The highest LOD score of 10.61 was observed for the *Di2* morphological marker, located at 49.9 cM in the same map position of SNP680499 and SNP681064. This QTL explains 40.2% of the additive phenotypic variance, supporting a tight relationship between DF and BD traits.

High-resolution mapping of q*BD6.1*

For increasing mapping resolution, segregation analyses were performed in WFPxP and two additional F2 populations, $WxBy^{C}$ and $WxBy^{D}$, derived from the F1 cross 'NJ Weeping' (homozygous DF) x 'Bounty' (SF). Considering the co-localization of q*BD6.1* with the *Di2* locus and the shared donor of the DF trait (i.e. 'Red Weeping') between 'Weeping Flower Peach' and 'NJ Weeping' seed parents, a common genetic factor(s) underlying q*BD6.1* was assumed among these progenies. Based on allelic patterns within the interval flanked by SNP680124 and SNP681888, a total of 10 recombinant individuals were identified, while the remaining were either heterozygous (genotype indicated as $BD6.1_{H}$) or homozygous ($BD6.1_{S}$ or $BD6.1_{P}$, respectively inherited from seed late-blooming/DF and pollen early-blooming/SF parent). Irrespective of the progeny or season, the relationship among genotype groups and BD was almost linear: $BD6.1_{P}$ flowered significantly earlier compared to $BD6.1_{H}$ (inter-progenies average delay of 5.4 days), which in turn bloomed earlier than $BD6.1_{S}$ (delay of 7.6 days) (**Figure 3A**). Clearly, BD was also linked to the DF trait, being $BD6.1_{P}$ all single-flower individuals, while $BD6.1_{S}$ and $BD6.1_{H}$ were homozygous and heterozygous DF, respectively. This relationship is particularly evident when correlating BD with the average number of supernumerary petals in $BD6.1_{S}$ and $BD6.1_{H}$ genotypes (**Supplemental Figure 3**). Interestingly, q*BD6.1* segregation was not associated with chilling requirement (i.e. the sum of hours with temperature between 0 - 7.2 °C) ranging from 835 to 1040 Chilling Hours (**Figure 3B)**, and conversely strictly correlated with heat-requirement, as GDH (i.e. the sum of Growing Degree Hours between 4.5 - 36 °C) for flowering proportionally increased from 4294 for $BD6.1_{P}$ to 5845 for $BD6.1_{S}$ (**Figure 3C**).

The magnitude of phenotypic effects among genotypic groups was large enough to map qBD6.1 as a Mendelian-like factor, allowing a confident tracking of meiotic recombination events (**Figure 4**). In WFPxP, recombinant individuals #069, #022 and #081 (ranging from 83 to 86 JD) flowered in the range of earliest blooming BD6.1$_P$ group (85±4 JD), while #066 (91 JD) in BD6.1$_H$ group (90±3 JD). This allows a first delimitation of q*BD6.1* to a region of about 200 Kb between SNP_IGA_680329 and SNP_IGA_681209 (24,006,441 – 24,200,807 bp). In WxBy progenies, BD of double-recombinant WxBy^C #028 (74±2 JD) was not significantly different from the BD6.1$_H$ group (72.1±2 JD, *p*-value 0.427), while WxBy^D #022 (83±3 JD) bloomed in the range of latest blooming BD6.1$_S$ group (82±2 JD, *p*-value 0.015). Other non-informative recombinants are shown in **Figure 4**. Additional markers designed within the target interval narrowed down the locus to an about 80 Kb region, comprised between BD6_097 and BD6_609 (24,019,097 – 24,104,609 bp): according to peach reference v2.1 transcript annotation, the corresponding physical interval contains 9 gene models (**Figure 4**).

Candidate gene(s) for BD within the fine-mapped interval

Genomic variants within the q*BD6.1* locus were identified by analyzing whole-genome re-sequencing data of W ('NJ Weeping') and By ('Bounty') parents. Putative causal mutations were prioritized by considering the incomplete dominance of q*BD6.1* QTL in F_2 progenies and the absence of BD segregation in F_1 WxBy individuals, both coherent with a homozygous variant inherited from W parent. After filtering by these selection criteria and visual inspection of BAM alignments, a total of 35 variants were found (**Supplemental File 1**), including a 994 bp deletion (hereafter named *pet$_{DEL}$*) previously found at C-terminus of *Prupe.6G242400* gene (encoding a PETALOSA TOE-type protein, Gattolin et al., 2018, 2020) (**Figure 4**). Apart from *pet$_{DEL}$*, none of the other variants was located in coding sequences: all were distributed in upstream or downstream regions. Annotation of other predicted ORFs in the fine-mapping interval did not uncover genes previously associated to blooming time in either model or non-model species. Transcripts of 4 out the 9 ORFs were not or barely detectable in flower bud tissues from either early or late blooming genotypes, at least in the two sampled stages of dormant buds after CR fulfilment and first flower opening. Also, no evident transcriptional trends emerged from gene expression analysis of the remaining 4 ORFs, excluding *Prupe.6G242400* for which differential expression was observed between BD6.1$_S$ or BD6.1$_P$ (**Supplemental Figure 4**).

Mutation of PET-miR172 recognition site affects flowering date in genome-edited tobacco plants

The well-known complexity of peach transformation hinders an intra-specific validation of PET gene function and the exact role of the *pet* variant in blooming date. Therefore, potential effects of PET mutations were explored in genome-edited tobacco (*Nicotiana tabacum* 'Kentucky' variety) plants. For this purpose, a self-pollinated T_1 individual heterozygous for a T nucleotide frame shift insertion within the core miR172 recognition site in a *NtPET* ortholog (*NtBENa*, XP_016482517) was used to generate a segregating population. After germination, a total of 136 plants were screened using an allele specific probe designed on the edited site, showing concordance with the expected 1:2:1 Mendelian ratio (chi-square 1.37). An equal number of six wild type (wt), homozygotes for PET mutation (PET_{hom}) and heterozygous individuals (PET_{het}) were selected for evaluating plant phenology, flowering date and flower morphology. During the vegetative phase, plants showed a homogeneous development without significant differences in node differentiation rate among genotypes (**Supplemental Figure 5**). Phytomer number at the first flower-bearing node was similar among tobacco genotypes; however, first flower opening in *wt* plants occurred 107±2.1 days after germination (DAG), while PET_{het} and PET_{hom} genotypes flowered at 111±2.4 and 117±2.7 DAG, respectively, coherently with an incomplete dominance of the PET mutated allele over *wt* (**Figure 5A**). Aside from the late-flowering phenotype, the PET mutation also caused alterations of flower morphology, whose severity was dependent on its zygosity. PET_{het} flowers exhibited similar sepals and corolla to their *wt* counterparts, while displaying various degrees of stamens into petaloid structures conversion. In PET_{hom} flowers the corolla was consistently shorter than in *wt*, with fused petals also showing sepaloid traits; each flower also had supernumerary (i.e. more than 5) petaloid stamens and a normal ovary (**Figure 5B**). Other than delayed flowering, the comparison of homozygous q*BD6.1*/pet_{DEL} peach genotypes with PET_{hom} tobacco flowers outlines remarkable morphological similarities: the differentiation of supernumerary floral organs; the presence of both petaloid stamens and sepaloid petals; outgrowth of pistil from the corolla before flower opening (**Figure 5C**).

Discussion

Reproductive phenology largely determines the distribution of a genotype across different environments, particularly for tree species, characterized by a perennial habitus and long-term exposure to climate variability (Sherman & Beckman, 2003). Exploitation of adaptive and resilience traits associated to flower phenology, blooming date, is crucial to ensure agronomic success in the future, considering the increasing frequency of extreme weather events occurring in many growing areas. Early blooming cultivars tend to be more exposed to

the risk of spring frost bud damage, while late blooming ones can exhibit irregular floral development and low fruit set due to warm temperature regimes along the flowering period (Luedeling, 2012). Recent climatic trends, moving toward an increase of winter temperatures and late frost returns, have determined a growing interest in variable traits associated with reproductive phenology (Atkinson et al., 2013; Augspurger, 2013).

In this work, BD was dissected in a peach collection including high- and low-CR accessions and located in a temperate area of northern Italy. Association analyses identified three major loci on chr. 4, 6 and 8 explaining most of the observed phenotypic variability for BD. The involvement of these genomic regions has been previously reported in different QTL mapping studies for BD in peach (Fan et al., 2010; Romeu et al., 2014; Bielenberg et al., 2015; Hernández Mora et al., 2017). However, in comparison with these studies, we recorded a limited range of BD variation (about 10 days) across the two monitored seasons, probably reflecting the typical climatic conditions of this environment: a moderately cold winter ensuring complete fulfillment of CR in high-chill accessions and a long winter tail of sub-optimal temperatures delaying HR accumulation in low-chill ones. The absence of signals for a region on chr. 1 previously reported as the major CR-related QTL affecting blooming in sub-tropical climate (Fan et al., 2010; Romeu et al., 2014) seems to support the hypothesis of a minor contribution of CR in more temperate environments.

Considering the presence of some DF accessions within the panel, the co-localization of q*BD6.1* signal with a known locus affecting flower morphology (*Di2*) was further investigated in various progenies segregating for both the *Di2* and BD traits. The strong phenotypic effect and the Mendelian-like inheritance allowed high-resolution mapping of q*BD6.1* to a small region of about 80 Kb overlapping the *Di2* locus. Whole-genome information along with gene expression analyses supported a prime candidate role for the 994 bp deletion (pet_{DEL}) variant at the C-terminus of *PETALOSA* (*PET*) gene (*Prupe.*6G242400) (Gattolin et al., 2018). The encoded protein belongs to the AP2/TOE class of transcription factors known to play a major role in floral transition (Yant et al 2010, Zhang et al 2015) as well as floral patterning, where they specify the B-function of floral organ identity in the ABCDE model proposed for Arabidopsis (Rijpkema et al., 2010, Krogan et al 2012). As recently elucidated in phylogenetically distant eudicots, natural variations affecting the C-terminal region and miR172 target site within the orthologous PET clade of TOE genes induce conserved modifications of flower morphology (Gattolin et al., 2020). However, potential effects of *pet* mutations on flowering time were not previously reported. Given the proven difficulties of peach transformation, genome-edited tobacco plants were used to provide insight into the role of PET mutations in flower phenology. Several layers of evidence

support the results deriving from genetic and genomic analyses in peach. Firstly, a single nucleotide insertion within the core PET-miR172 recognition site was sufficient to induce a late-flowering phenotype in tobacco. Secondly, the segregation analysis of this PET mutant allele showed an incomplete dominance over the *wt* allele, resulting in a more delayed flowering in PET_{hom} lines compared to PET_{het}; the same pattern also characterizes q*BD6.1*/pet_{DEL} inheritance in peach, as homozygous pet_{DEL} genotypes bloom later compared to the heterozygote. Beside flowering time, additional layers of evidence were provided by the range of pleiotropic effects induced in floral patterning: in tobacco, the PET mutation causes weak to severe alteration of flower morphology depending on the allelic status (as evident in the PET_{hom} line). Remarkably, these effects were also observed in peach, where the development of supernumerary organs, petaloid stamens and sepaloid petals were particularly evident in homozygous pet_{DEL} genotypes. Therefore, despite the phylogenetic distance between Rosaceae and Solanaceae, the resemblance of phenological and morphological traits strongly supports a conserved function of *PET* genes in regulating floral timing and patterning, and a role for the q*BD6.1*/pet_{DEL} as a *bona fide* variant in peach blooming date.

These findings are also supported by increasing evidence for the role of the miR172-AP2/TOE module in the control of the vegetative-to-reproductive transition and floral patterning in both annual and perennial plants (Wang, 2014, Debernardi et al., 2017, Aukerman and Sakai 2003). In the tree species *Jatropha curcas*, the overexpression of miR172 not only resulted in early flowering but caused the abnormal development of reproductive organs (Tang et al., 2018). In apple lines over-expressing miR172, different transgene expression levels cause a range of flower alterations and fruit size reduction (Yao et al., 2015). However, while miR172 overexpression studies point to the miRNA-dependent AP2/TOE gene regulation as the mechanism underlying these phenotypes, some functional aspects related to the allelic variation at C-terminus regions of these genes remain to be elucidated, as natural or artificially induced mutations also affect protein aminoacidic sequence. In contrast, the knowledge on molecular mechanisms behind temperature-mediated regulation of blooming time, as well as genetic determinants underlying cold and heat-requirements are scarcely known in fruit tree species. In Arabidopsis, SHORT VEGETATIVE PHASE (SVP) plays an important role in the response of plants to ambient temperature changes, controlling flowering time by negatively regulating the expression of FT (Lee et al., 2007). Interestingly, this MADS box gene is phylogenetically related to the *DORMANCY-ASSOCIATED MADS-BOX* (*DAM*), co-locating with the non-dormant EVG mutant in peach (Bielenberg et al., 2008) and major candidates for the control of bud dormancy in numerous fruit species (Falavigna et al., 2019). In this work, the tight

association with GDH accumulation for flowering, in contrast to the lack of significant differences for CR, provide a convincing evidence of *pet*$_{DEL}$ variant as a major QTL determinant for heat-requirement, also suggesting a role for the miR172-TOE route (and associated genetic variations) in temperature-dependent regulation of blooming in a fruit tree species. In Arabidopsis, miR156 and miR172 seem to be involved in thermosensory flowering time pathway, as their abundance is regulated in an opposite manner in plants grown at 16 or 23 ºC (Lee et al., 2010). Whether these miRNAs affect the speed of developmental progress at different temperatures, as well as the precise molecular framework remain to be elucidated. Interestingly, the PET mutation does not alter tobacco vegetative development, as supported by the lack of a significant difference in phytomer number at the first flower-bearing node. Rather, it might cause a prolonged growth of floral buds, which appeared to take longer to develop prior to opening in PET$_{hom}$ compared to wt. Similarly, in peach, the total number of petals tends to be positively correlated with BD, supporting the hypothesis of a temporal extension of bud meristem activity, in turn determining an increased HR for progressing through each flower phenophase.

Some interesting aspects remain to be clarified on this matter, first and foremost whether the development of extra-numerary organs in peach is pre-determined before the endo-dormancy induction. In peach, the anatomical development of flower buds continues throughout the dormancy period, although the growth of whorls strongly slows down during winter (Reinoso et al., 2002); the rapid maturation phase only occurs in late winter and continues through early spring, after completion of vascular connections between flower primordia and branch wood (Reinoso et al., 2002). In sweet cherry, growth arrest of flower buds occurs consistently at the same stage of flower development (characterized by the presence of all differentiated whorls), resulting in attenuated differences among cultivars (Fadón et al., 2018).

In summary, a major QTL for heat-requirement affecting blooming date was characterized in peach. Genetic analyses together with proof-of-concept validation in an engineered annual model plant, allow the prioritization of a candidate variant in a PETALOSA gene clade previously linked to alteration of flower morphology. The extent of the phenotypic effect of *qBD6.1* and its simple genetic inheritance could be relevant for improving reproductive phenology in peach, particularly considering the rather limited range of BD variability observed in our collection panel and latitude. This variant has potential applications for improving phenological plasticity and adaptation to the environment, particularly relevant for peach and other stone fruits.

Materials and Methods

Plant material

The panel used for GWAS includes a total of 133 accessions characterized by a wide range of CR (from 50 - 1100 CU). The collection is located in the experimental farm 'M. Neri' (Imola, Bologna, Italy). Three peach F2 progenies were used in this work: WFP×P, composed of 381 individuals deriving from the cross S2678 ('Weeping Flower Peach') × S6146 ('Pamirskij 5'), located in Avignon Domaine Experimental des Garrigues (INRA, France); two progenies derived from the self-pollination of F1 seedlings from the cross 'PI91459' ('NJ Weeping') × 'Bounty', W×By^{C} and W×By^{D} composed of 37 and 61 individuals, respectively, both located in the experimental field of the University of Milan, Azienda Didattico Sperimentale F. Dotti (Lodi, Italy).

Phenotyping

Blooming date (BD) was visually scored as the date at which 50% of the floral buds on an individual tree reached complete opening and recorded as the number of days from January 1st of each year (Julian Days, JD). Bloom progression was monitored every 3 days from the onset of floral bud break. BD was recorded in the collection panel of 133 accessions in years 2012 and 2013 (100 accessions common to both years of evaluation) (**Supplemental Table 1**); in 2013 in F_2 WFPxP individuals and in 2019/2020 in W×By progenies. The double-flower trait was scored as a qualitative phenotype. Morphological observation and quantitative data about sepal, petal and stamen numbers were also collected. Chilling requirement (CR) was determined following the method of Gibson and Reighard (2002). Briefly, medium vigor shoots were harvested on a weekly basis from the beginning of January; cuttings were put in a 5% sucrose:water solution and placed in a 20 °C growth chamber maintained under a 16/8 hour photoperiod; CR was considered to be fulfilled when visible petals opened in at least of 50% of the flower buds on all cuttings and calculated using the Chill Hours (CH) model (Weinberger, 1950). Heat-requirement (HR) was estimated using the model proposed by Richardson et al. (1974), which calculates Growing Degree Hours (GDH) as the sum of hourly temperatures between 4.5 and 36 °C. Temperature measurements for CR and HR calculation were provided by a nearby weather station.

Genome-wide association analysis

IPSC peach 9 K SNP array genotyping data were filtered for marker missing rate lower than 10% and minor allele frequency higher than 5%, finally retaining a total of 6,049 SNPs for GWAS (Micheletti et al., 2015). The peach genome assembly V2.0 was used as a reference for SNP marker positions. The Fixed and random model Circulating Probability Unification

(FarmCPU) method (Liu et al., 2016) was used for association analysis, using the 2 components from PCA as covariates to account for population structure (previously reported in Cirilli et al., 2018). The performance of was evaluated by comparing the observed vs. expected p-values under null hypothesis, through quantile-quantile (QQ)-plot inspection. A conservative threshold for assessing SNP significance was set based on Bonferroni correction for a type I error rate of 0.01 or using a permutation threshold calculated using MVP package. Intra-chromosomal LD patterns were measured and visualized using HAPLOVIEW v4.2.

Crossing populations genotyping and fine mapping

The F2 progeny WFP×P was genotyped using the 9K International Peach SNP Consortium (IPSC) SNP array v1, recalibrated based on Peach Reference Genome v2.0 (Verde et al., 2017). High-density linkage map of WFP×P build by Mauroux et al., (2013) were used for QTL analysis, using interval mapping algorithm implemented in MapQTL 6.0 software package. The segregation pattern of the double-flower trait was also included as a dominant marker (Di2 and di2 for double and single flowers, respectively). Genomic variants and segregating SNPs around the q*BD6.1* locus were identified from whole genome re-sequencing data of W and By parents available under SRA BioProject archive PRJNA479850, following the workflow described by Cirilli et al. (2018). Sequences of primers used for fine mapping are reported in **Supplemental Table 2**. For fine-mapping, SNP variants were genotyped using a high-resolution melting (HRM) analysis-based approach. HRMA was carried out in a QuantStudio 3 Real-Time PCR System (Thermo-Fisher) using PowerUp SYBR Green Master mix (Applied biosystems). Reactions were carried out with the following thermal program: 2 min at 94 °C, 40 cycles of 30 s at 94 °C, 30 s annealing at 58 °C and 30 s at 72 °C, followed by a melting step over a 70 - 95 °C gradient with 0.1 °C s^{-1} ramp rate. Data were analyzed using the QuantStudio 3 software v1.3 and visualized using both a derivative and difference plot, according to the software instructions.

qPCR expression analysis

Tissues were collected from flower buds at the developmental stages of inflorescence buds swelling (BBCH stage 51) and sepals opening (BBCH stage 57). For qPCR, total RNA was extracted from bud tissues using a RNeasy kit (Qiagen) and cDNA synthesized by One-Step RT-PCR kit (Qiagen) using oligo-dT primers, according to manufacturer's instructions. Transcript and related specific primers are listed in Table S2. The relative gene expression level was calculated using the comparative delta-CT method with Actin transcript (*Prupe.6G163400*) as internal reference control. Three biological replicates were analyzed for each sample.

Screening of T2 CrispR-Cas9 tobacco plants

CrispR-Cas9 editing of tobacco plants for PETALOSA gene was previously described (Gattolin et al., 2020). Briefly, Nicotiana tabacum cv TI 527 'Kentucky' plants were transformed with a c58 Agrobacterium strain armed with the binary vector pHAtC targeting the core miR172 binding site within PETALOSA orthologs NtBENa (XP_016482517) and NtBENb (XP_016499635). The absence of the transgene was assessed using Left and Right Borders specific primers for the T-DNA sequence. Target-specific mutations in T1 plants were assessed by Sanger sequencing of PCR fragments. A T1 line bearing a heterozygous T insertion within the core miR172 binding site of NtBENa was self-pollinated and segregation of T2 plants were screened using HRMA assay. Specific primers were designed to selectively amplify *BENa* and *BENb* genes. Edited site was than screened in *BENa* fragments flanking the PAM recognition sequence within the miR172 target site of PET target genes (**Supplemental Table 2**). HRM analysis was carried out as previously described in the paragraph above.

Acknowledgements

We are grateful to Emanuele Quattrini, Martina Lama and Stefano Foschi for technical assistance in the field. This work has been partially funded by the EU seventh framework program FruitBreedomics project (grant no. FP7-265582): Integrated approach for increasing breeding efficiency in fruit tree crops (genotyping of most of the accessions). The views expressed in this work are the sole responsibility of the authors and do not necessarily reflect the views of the European Commission. The work was partly supported by FREECLIMB project, and, at the University of Milan also partially funded in the framework of MAS.PES (Italian project aimed at apricot and peach breeding funded by Italian growers' and nurseries' organizations http://www.maspes.org/).

Disclosures

The authors have no conflicts of interest to declare

Author Contributions

MC conceived the work, performed genotyping and phenotyping, and drafted the manuscript. SG developed tobacco engineered lines and performed phenotypic analysis, revised the manuscript; RC and IB helped with genotypic and phenotypic analyses; BQ and TP provided data of WFP×P progeny; LR and DB coordinated and conceived the study, critically revised the manuscript for important intellectual content. All authors read and approved the final version of the manuscript.

Figures and Tables legends

Figure 1. A) Frequency distribution of blooming date (BD), in the two evaluated year, expressed as Julian Days (JD) in the peach collection panel of 133 accessions; B) Manhattan plot and C) QQ-plots of -log10p-values estimated for BD trait using FarmCPU model adjusted for population structure. Horizontal lines indicate the Bonferroni-adjusted threshold (violet) and permutation tests for year 2012 (dashed light grey) and 2013 (dashed purple).

Figure 2. A) Frequency distribution of blooming date (BD) in WFP×P progeny; B) Location of q*BD6.1* QTL on integrated map of chromosome 6 associated to BD in WFP×P progeny. Genetic distances (in centimorgans, cM) and LOD score for QTL significance are shown. Di2 indicate DF morphological marker.

Figure 3. Association between allelic status at qBD6.1 locus ($BD6.1_S$ indicates genotypes with both alleles inherited from seed late-blooming/DF parent; $BD6.1_P$ with both allele inherited from pollen early-blooming/SF parent; $BD6.1_H$ heterozygous) and A) Blooming Date (BD, in Julian Days) in the three progenies WFP×P, W×By^C and W×By^D, B) Chilling Requirement (CR, in Chilling Hours) and C) Heat Requirement (HR, in Growing Degree Hours) in the progeny WxBy^D.

Figure 4. Meiotic recombination events detected at q*BD6.1* locus. BD of each recombinant individuals and respective blooming group averages: $BD6.1_S$ both alleles inherited from seed late-blooming/DF parent; $BD6.1_P$ both alleles inherited from pollen early-blooming/SF parent; $BD6.1_H$ heterozygous). Gene models annotated in the fine-mapped physical interval and the PETALOSA deletion (petDEL) on transcript (Prupe.6G242400) are also shown.

Figure 5. A) Flowering date in heterozygous (PET_{het}) and homozygous (PET_{hom}) tobacco plants carrying a nucleotide insertion within the miR172 core recognition site at the C-terminus of PETALOSA gene *NtBENa* (XP_016482517), as compared to *wt* control plants. The three genotypes (*wt*, PET_{het} and PET_{hom}) derived from the segregation of a single T1 heterozygous individual. B) Morphological evaluation of PET_{het} and PET_{hom} tobacco flowers. C) Comparison of flower morphology in SF BD6.1P (a, b) and DF BD6.1S (c – f), carrying the homozygous pet_{DEL} variant) peach individuals, DF individuals are characterized by the presence of a longer peduncle (d), petaloid stamens (e) and sepaloids petals (f).

Table 1. Statistical information on associated SNPs from GWAS analysis for BD.

Supplementary material

Supplemental Figure 1. Linkage disequilibrium pattern around the q*BD6.1* locus on chromosome 6. Most associated SNPs from GWAS and the position of *Di2* locus are shown.

Supplemental Figure 2. Single-marker QTL analyses for BD in WFP×P progeny.

Supplemental Figure 3. Pearson's correlation between Blooming Date (BD, in Julian Days) and the average number of supernumerary petals in DF genotypes $BD6.1_S$ (alleles inherited from seed late-blooming parent) and $BD6.1_H$ (heterozygous) in WFP×P and W×By^D progenies.

Supplemental Figure 4. Real-time PCR analysis of transcripts annotated in the qBD6.1 fine-mapped intervals as resulted from the comparison of $BD6.1_S$ (alleles inherited from seed late-blooming/DF parent) and $BD6.1_P$ (alleles inherited from pollen early-blooming/SF parent)) genotypes. Three different individuals for each genotype were used as biological replicates. In flower buds tissue at the developmental stages of inflorescence buds swelling (pre-bloom, BBCH 51) and sepals opening (bloom, BBCH stage 57). Asterisks indicate statistical significance difference (Tukey test, $p < 0.01$).

Supplemental Figure 5. Dynamics of tobacco growth in terms of number of differentiated phytomers assessed every 2 weeks from germination.

Supplemental Table 1. List of accessions used in this study. Blooming date (BD) was recorded during seasons 2012 and 2013 and expressed in Julian Days (JD). Double-flower accessions are underlined.

Supplemental Table 2. List of primers used in this study.

Supplemental File 1. Full list of variants annotations and effects (as calculated with SNPEff tool) from whole genome sequencing assembly of NJ Weeping and Bounty parents 1 on fine-mapped q*BD6.1* interval. See text for variants filtering criteria.

References

Andres F, Coupland G. The genetic basis of flowering responses to seasonal cues. Nature Reviews Genetics. 2012;13(9):627–639

Atkinson CJ , Brennan RM, Jones HG (2013) Declining chilling and its impact on temperate perennial crops. Environ Exp Bot 91:48–62

Augspurger, C. K. (2013). Reconstructing patterns of temperature, phenology, and frost damage over 124 years: spring damage risk is increasing. Ecology 94, 41–50

Bielenberg, D. G., Wang, Y., Fan, S., Reighard, G. L., Scorza, R., Abbott, A. G. (2004). A deletion affecting several gene candidates is present in the Evergrowing peach mutant. J. Hered. 95, 436–444

Castède, S., Campoy, J. A., Le Dantec, L., Quero-García, J., Barreneche, T., Weden, B., et al. (2015). Mapping of candidate genes involved in bud dormancy and flowering time in sweet cherry (Prunus avium). PloS One 10 (11), e0143250.

Chmielewski, F. M., Gotz, K. P., Homann, T., Huschek, G., Rawel, H. M. (2017). Identification of endodormancy release for cherries (Prunus Avium L.) by abscisic acid and sugars. J. Hortic. 4, 3

Cirilli M, Giovannini D, Ciacciulli A, Chiozzotto R, Gattolin G, Rossini L et al (2018) Integrative genomics approaches validate PpYUC11-like as candidate gene for the stony hard trait in peach (P. persica L. Batsch). BMC Plant Biol 18:88

Cirilli, M., Flati, T., Gioiosa, S. et al. (2018) PeachVar-DB: a curated collection of genetic variations for the interactive analysis of peach genome data. Plant Cell Physiol. 59, e2.

Couvillon GA, Erez A. 1985. Influence of prolonged exposure to chilling temperatures on bud break and heat requirement for bloom of several fruit species. Journal of the American Society for Horticultural Science 110: 47– 50.

J.M. Debernardi, H. Lin, G. Chuck, J.D. Faris, J. Dubcovsky (2017) microRNA172 plays a crucial role in wheat spike morphogenesis and grain threshability Development, 144 (2017), pp. 1966-1975

Dennis, E. S., & Peacock, W. J. (2007). Epigenetic regulation of flowering. Current Opinion in Plant Biology, 10(5), 520–527

Dirlewanger, E., Quero-García, J., Le Dantec, L., Lambert, P., Ruiz, D., Dondini, L., et al. (2012). Comparison of the genetic determinism of two key phenologycal traits, flowering and maturity dates, in three Prunus species: peach, apricot and sweet cherry. Hered 109, 280–292.

Engin, H.; Ünal, A. Examination of flower bud initiation and differentiation in sweet cherry and peach by scanning electron microscope. Turk. J. Agric. For. 2007, 31, 373–379.

Fan S, Bielenberg DG, Zhebentyayeva TN, Reighard GL, Okie WR, Holland D, Abbott AG: Mapping quantitative trait loci associated with chilling requirement, heat requirement and bloom date in peach (Prunus persica). New Phytol 2010, 185:917–93

Fadón, E.; Herrero, M.; Rodrigo, J. Flower bud dormancy in Prunus species. In Advances in Plant Dormancy; Anderson, J.V., Ed.; Springer: Cham, Switzerland, 2015; pp. 123–135

Fadón, E., Rodrigo, J., Herrero, M. (2018). Is there a specific stage to rest? Morphological changes in flower primordia in relation to endodormancy in sweet cherry (Prunus avium L.). Trees 32, 1583–1594

Fadón, E.; Herrera, S.; Guerrero, B.I.; Guerra, M.E.; Rodrigo, J. Chilling and Heat Requirements of Temperate Stone Fruit Trees (Prunus sp.). Agronomy 2020, 10, 409.

Fishman, S.; Erez, A.; Couvillon, G.A. The temperature dependence of dormancy breaking in plants: Mathematical analysis of at two-step model involving a cooperative transition. J. Theor. Biol. 1987, 124, 473–483.

Gattolin S, Cirilli M, Pacheco I, et al. 2018. Deletion of the miR172 target site in a TOE-type gene is a strong candidate variant for dominant double-flower trait in Rosaceae. The Plant Journal 96, 358–371.

Gattolin, S, Cirilli M, Chessa S, et al. 2020. Mutations in orthologous PETALOSA TOE-type genes cause dominant double-flower phenotype in phylogenetically distant eudicots. Journal of Experimental Botany 71, 2585–2595.

Gibson PG, Reighard GL. 2002. Chilling requirement and postrest heat accumulation in peach trees inoculated with peach latent mosaic viroid. Journal of the American Society for Horticultural Science

Guo, L.; Dai, J.; Ranjitkar, S.; Yu, H.; Xu, J.; Luedeling, E. Chilling and heat requirements for flowering in temperate fruit trees. Int. J. Biometeorol. 2014, 58, 1195–1206.

Hernández Mora JR, Micheletti D, Bink M, Van de Weg E, Bassi D, Nazzicari N et al (2017) Integrated QTL detection for key breeding traits in multiple peach progenies. BMC Genomics 18(1):404.

Krogan NT, Hogan K, Long JA. 2012. APETALA2 negatively regulates multiple floral organ identity genes in Arabidopsis by recruiting the co-repressor TOPLESS and the histone deacetylase HDA19. Development 139, 4180-90.

Horvath, D. P., Anderson, J. V., Chao, W. S., Foley, M. E. (2003). Knowing when to grow: signals regulating bud dormancy. Trends Plant Sci. 8, 534–540 B.A.

Krizek, J.C. Fletcher. Molecular mechanisms of flower development: an armchair guide Nat. Rev. Genet., 6 (2005), pp. 688-698

Lang, A. G., Early, J. D., Martin, G. C., Darnell, R. L. (1987). Endo-, para- and ecodormancy: Physiological terminology and classification for dormancy research. HortScience 22, 371–377

Li, Z., Reighard, G. L., Abbott, A. G., Bielenberg, D. G. (2009). Dormancy-associated MADS genes from the EVG locus of peach [Prunus persica (L.) Batsch] have distinct seasonal and photoperiodic expression patterns. J. Exp. Bot. 60, 3521–3530

Liu X, Huang M, Fan B, Buckler ES, Zhang Z. Iterative usage of fixed and random effect models for powerful and efficient genome-wide association studies. PLoS Genet. 2016;12(2):e1005767.

Luedeling, E.; Brown, P.H. A global analysis of the comparability of winter chill models for fruit and nut trees. Int. J. Biometeorol. 2011, 55, 411–421. [CrossRef] [PubMed].

Luedeling, E. (2012). Climate change impacts on winter chill for temperate fruit and nut production: a review. Sci. Hortic. 144, 218–229.

Mauroux, J.B., Quilot-Turion, B., Pascal, T., Dirlewanger, E., Campoy-Corbalan, J.A., Troggio, M., Verde, I., Micheletti, D., Aranzana, M.J. and Lambert, P. (2013) Building high-density peach linkage maps based on the ISPC 9K SNP chip for mapping Mendelian traits and QTLs: benefits and drawbacks. Acta Hortic. 1, 113– 118.

Michaels SD, Amasino RM (1999) FLOWERING LOCUS C encodes a novel MADS domain protein that acts as a repressor of flowering. Plant Cell, 11 (5): 949–56

Micheletti D, Dettori MT, Micali S, Aramini V, Pacheco I, Da Silva Linge C, et al. Whole-genome analysis of diversity and SNP-major gene association in peach germplasm. PLoS One. 2015;10:e0136803.

Olukolu, B. A., Trainin, T., Fan, S., Kole, C., Bielenberg, D. G., Reighard, G. L., et al. (2009). Genetic linkage mapping for molecular dissection of chilling requirement and budbreak in apricot (Prunus armeniaca L.). Genome 52 (10), 819–828.

Okie, W.R.; Blackburn, B. Increasing chilling reduces heat requirement for floral budbreak in peach. HortScience 2011, 46, 245–252

Quilot, B., Wu, B. H., Kervella, J., Génard, M., Foulongne, M., Moreau, K. (2004). QTL analysis of quality traits in an advanced backcross between Prunus persica cultivars and the wild relative species P. davidiana. Theor. Appl. Genet. 109, 884–897.

Reinoso, H., Luna, V., Pharis, R. P., Bottini, R. (2002). Dormancy in peach (Prunus persica) flower buds. V. Anatomy of bud development in relation to phenological stage. Can. J. Bot. 80, 656–663

Richardson, E.A.; Seeley, S.D.; Walker, D.R. (1974) A model for estimating the completion of rest for “Redhaven” and “Elberta” peach trees. HortScience, 9, 331–332 29

Romeu, J. F., Monforte, A. J., Sanchez, G., Granell, A., Garcia-Brunton, J., Badenes, M. L., et al. (2014). Quantitative trait loci affecting reproductive phenology in peach. BMC Plant Biol. 14, 52

Sánchez-Pérez, R., Dicenta, F., Martinez-Gomez, P. (2012). Inheritance of chilling and heat requirements for flowering in almond and QTL analysis. Tree Genet. Genomes 8 (2), 379–389.

Sherman WB, Beckman TG. 2003. Climatic adaptation in fruit crops. Acta Horticulturae 622: 411–428

Srikanth A. and Schmid M. Regulation of flowering time: all roads lead to Rome. Cell Mol. Life Sci. 2011; 68: 2013-2037

Tang M, Bai X, Niu LJ, Chai X, Chen MS, Xu ZF (2018) miR172 regulates both vegetative and reproductive development in the perennial woody plant Jatropha curcas. Plant Cell Physiol 59:2549–2563

Verde, I., Jenkins, J., Dondini, L. et al. (2017) The Peach v2.0 release: high-resolution linkage mapping and deep resequencing improve chromosome-scale assembly and contiguity. BMC Genomics, 18, 225.

Weinberger, J.H. Chilling requirements of peach varieties. Proc. Am. Soc. Hortic. Sci. 1950, 56, 122–128.

Warriner, C.L., J.L. Johnson and M.W. Smith. 1985. Comparison of the initiation and development of ‘Redhaven’ peach flowers in standard and meadow orchard trees. J. Amer. Soc. Hort. Sci. 110: 379-383

Wells, C. E., Vendramin, E., Jimenez Tarodo, S., Verde, I. & Bielenberg, D. G. A genome-wide analysis of MADS-box genes in peach [Prunus persica (L.) Batsch]. BMC Plant Biol. 15, 41 (2015)

Yant L, Mathieu J, Dinh TT, Ott F, Lanz C, Wollmann H, Chen X, Schmid M. 2010. Orchestration of the floral transition and floral development in Arabidopsis by the bifunctional transcription factor APETALA2. The Plant Cell, 22, 2156–2170.

Yu J, Conrad AO, Decroocq V, Zhebentyayeva T, Williams DE, Bennett D, Roch G, Audergon J-M, Dardick C, Liu Z, Abbott AG and Staton ME (2020) Distinctive Gene Expression Patterns Define Endodormancy to Ecodormancy Transition in Apricot and Peach. Front. Plant Sci. 11:180.

Zhebentyayeva, T. N., Fan, S., Chandra, A., Bielenberg, D. G., Reighard, G. L., Okie, W. R., et al. (2014). Dissection of chilling requirement and bloom date QTLs in peach using a whole genome sequencing of sibling trees from an F2 mapping population. Tree Genet. Genomes 10, 35–51

Zhang B, WangL, Zeng L, Zhang C, Ma H. 2015. Arabidopsis TOE proteins convey a photoperiodic signal to antagonize CONSTANS and regulate flowering time. Genes & Development29, 975–987.

Zhang X, An L, Nguyen TH, Liang H, Wang R, Liu X, et al. The cloning and functional characterization of peach *CONSTANS* and *FLOWERING LOCUS T* homologous genes *PpCO* and *PpFT*. PLoS One. 2015;10:e0124108

Zhang, Z., Zhuo, X., Zhao, K., Zheng, T., Han, Y., Yuan, C., et al. (2018). Transcriptome profiles reveal the crucial roles of hormone and sugar in the bud dormancy of prunus mume. Sci. Rep. 8, 5090.

Genome-wide association

Marker	chr	position (bp)	*p*-value	r^2
		BD2012		
SNP_IGA_381543	4	2,417,376	8.73e-05‡	0.26
SNP_IGA_682343	6	24,569,464	2.53e-04‡	0.10
SNP_IGA_873803	8	17,491,608	3.23e-06†	0.13
		BD2013		
SNP_IGA_386778	4	4,306,535	4.99e-07†	0.20
SNP_IGA_682704	6	24,651,810	4.00e-08†	0.11
SNP_IGA_877294	8	18,438,875	2.77e-06†	0.13

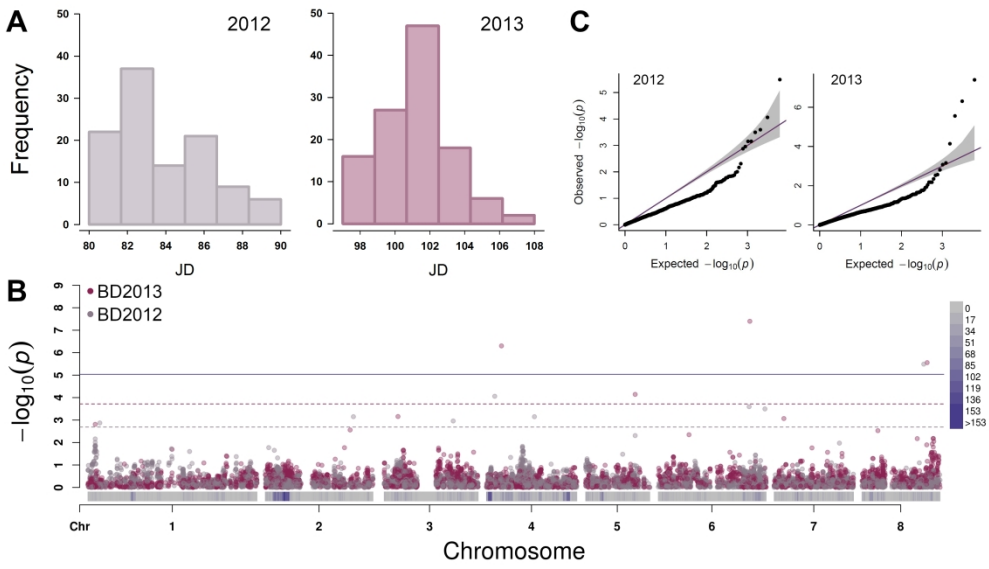

Figure 1. A) Frequency distribution of blooming date (BD), in the two evaluated year, expressed as Julian Days (JD) in the peach collection panel of 133 accessions; B) Manhattan plot and C) QQ-plots of -log10p-values estimated for BD trait using FarmCPU model adjusted for population structure. Horizontal lines indicate the Bonferroni-adjusted threshold (violet) and permutation tests for year 2012 (dashed light grey) and 2013 (dashed purple).

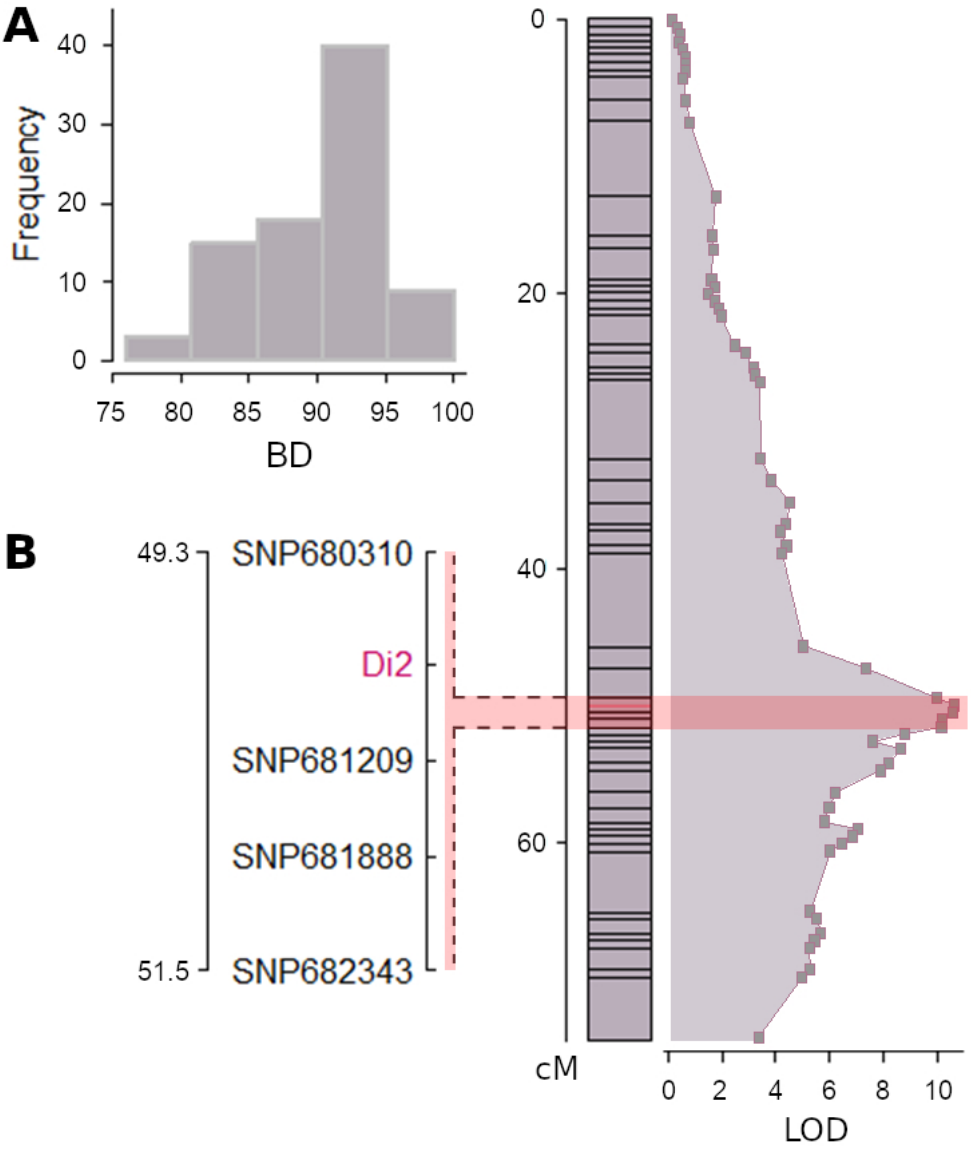

Figure 2. A) Frequency distribution of blooming date (BD) in WFP×P progeny; B) Location of qBD6.1 QTL on integrated map of chromosome 6 associated to BD in WFP×P progeny. Genetic distances (in centimorgans, cM) and LOD score for QTL significance are shown. Di2 indicate DF morphological marker.

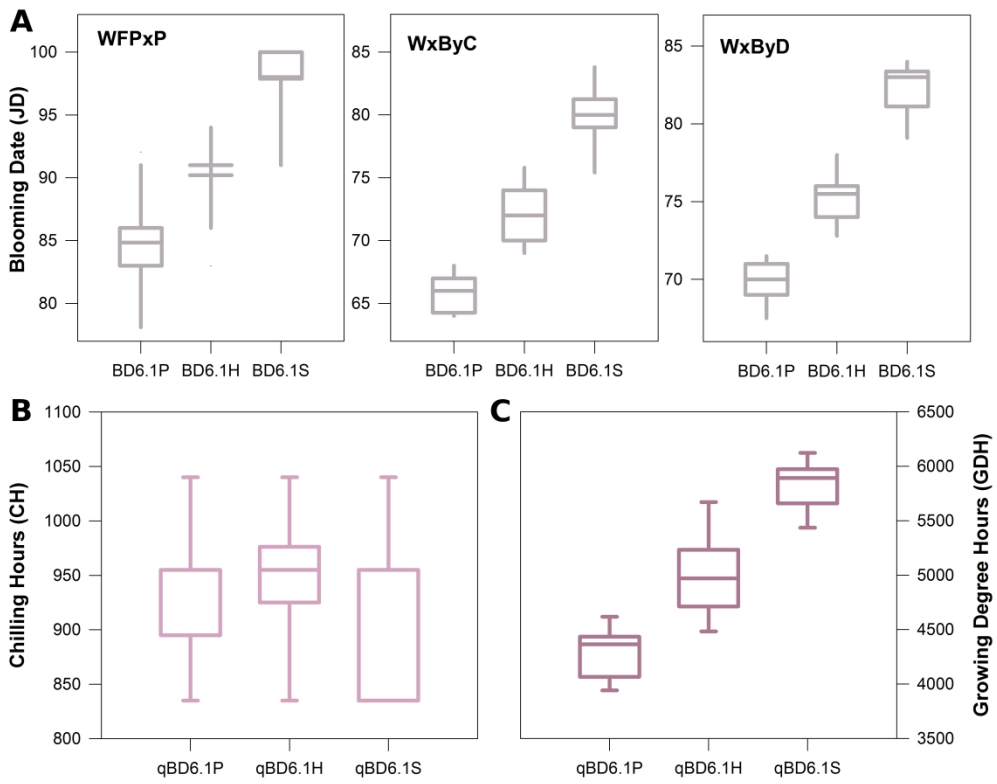

Figure 3. Association between allelic status at qBD6.1 locus (BD6.1S indicates genotypes with both alleles inherited from seed late-blooming/DF parent; BD6.1P with both allele inherited from pollen early-blooming/SF parent; BD6.1H heterozygous) and A) Blooming Date (BD, in Julian Days) in the three progenies WFP×P, W×ByC and W×ByD, B) Chilling Requirement (CR, in Chilling Hours) and C) Heat Requirement (HR, in Growing Degree Hours) in the progeny WxByD.

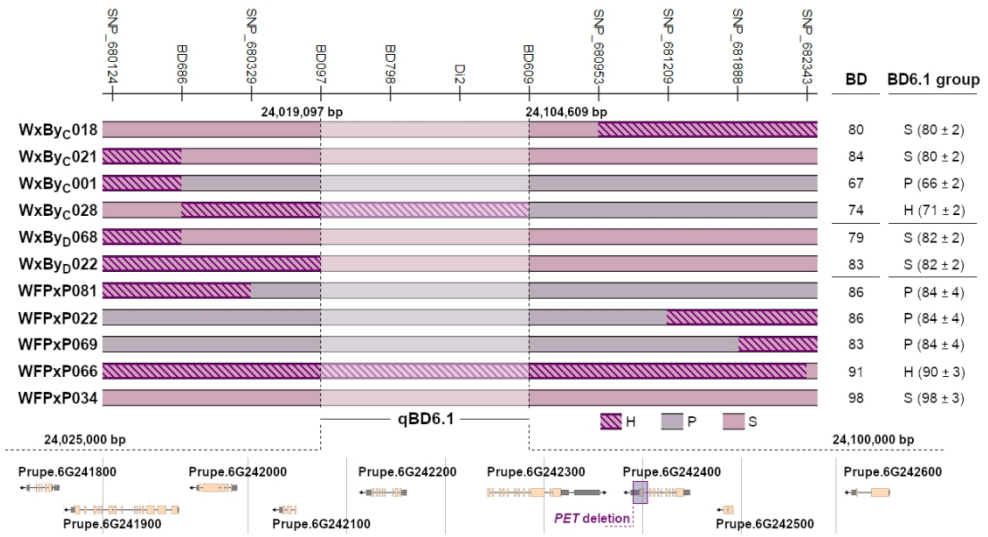

Figure 4. Meiotic recombination events detected at qBD6.1 locus. BD of each recombinant individuals and respective blooming group averages: BD6.1S both alleles inherited from seed late-blooming/DF parent; BD6.1P both alleles inherited from pollen early-blooming/SF parent; BD6.1H heterozygous). Gene models annotated in the fine-mapped physical interval and the PETALOSA deletion (petDEL) on transcript (Prupe.6G242400) are also shown.

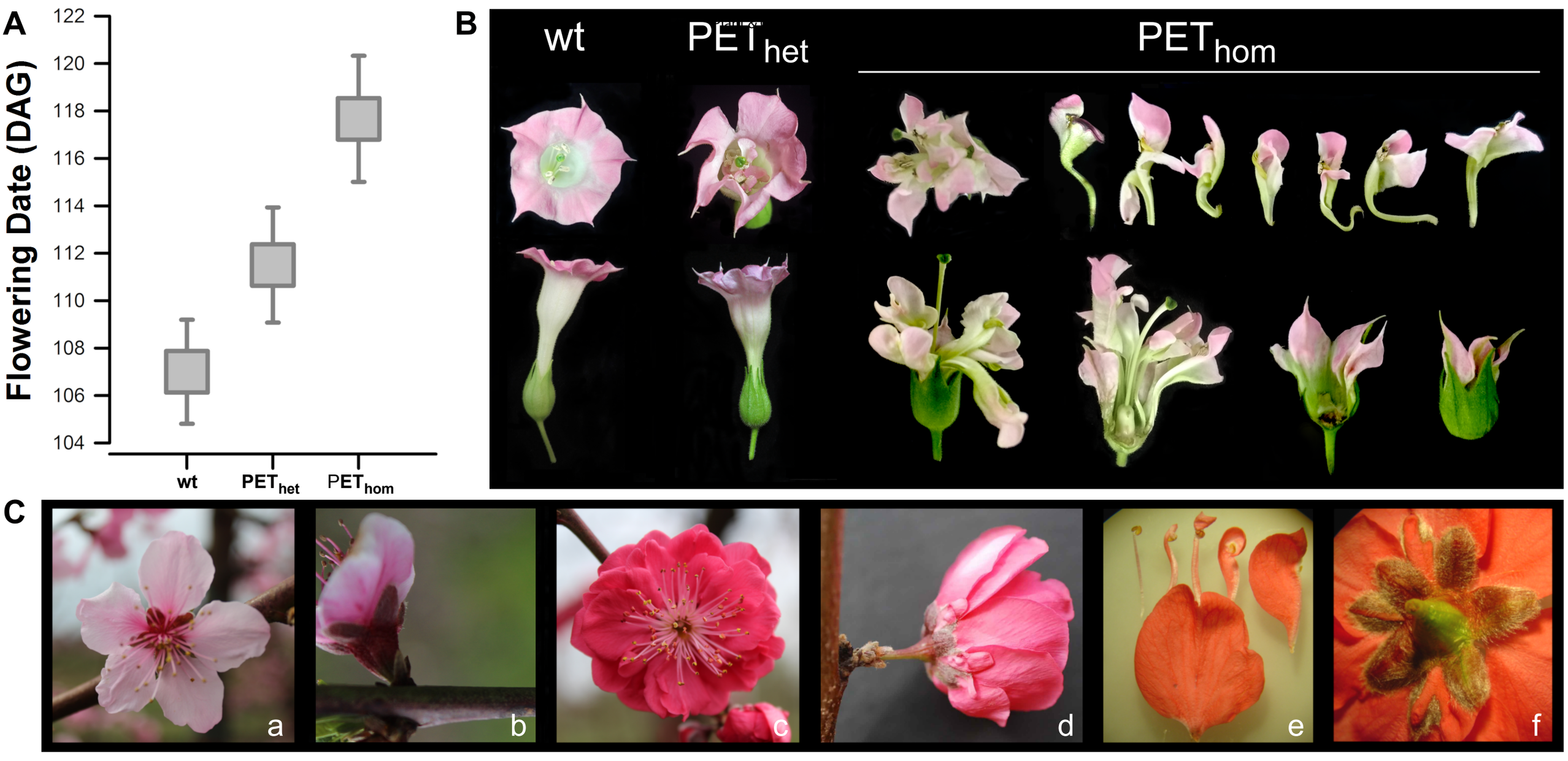
A
Flowering Date (DAG)
122
120
118
116
114
112
110
108
106
104
wt
PET het
PET hom
B
wt
PET het
PET hom
C
a
b
c
d
e
f

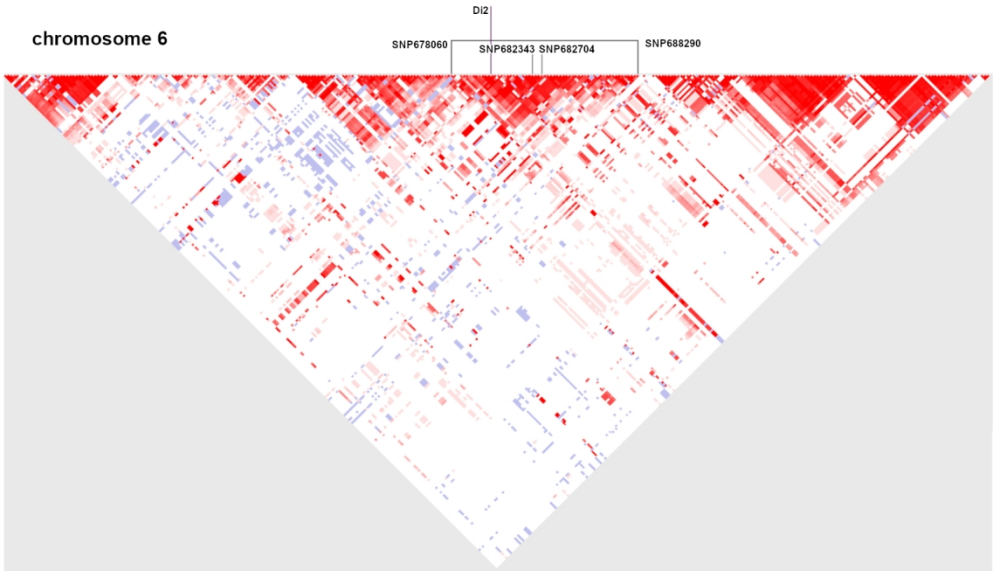
chromosome 6
Di2
SNP678060
SNP682343
SNP682704
SNP688290

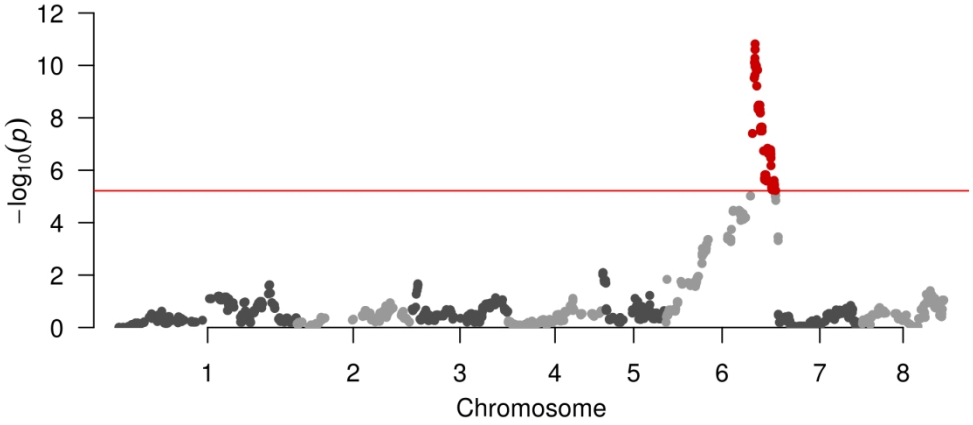
12
10
8
6
4
2
0
$-\log_{10}(p)$
1
2
3
4
5
6
7
8
Chromosome

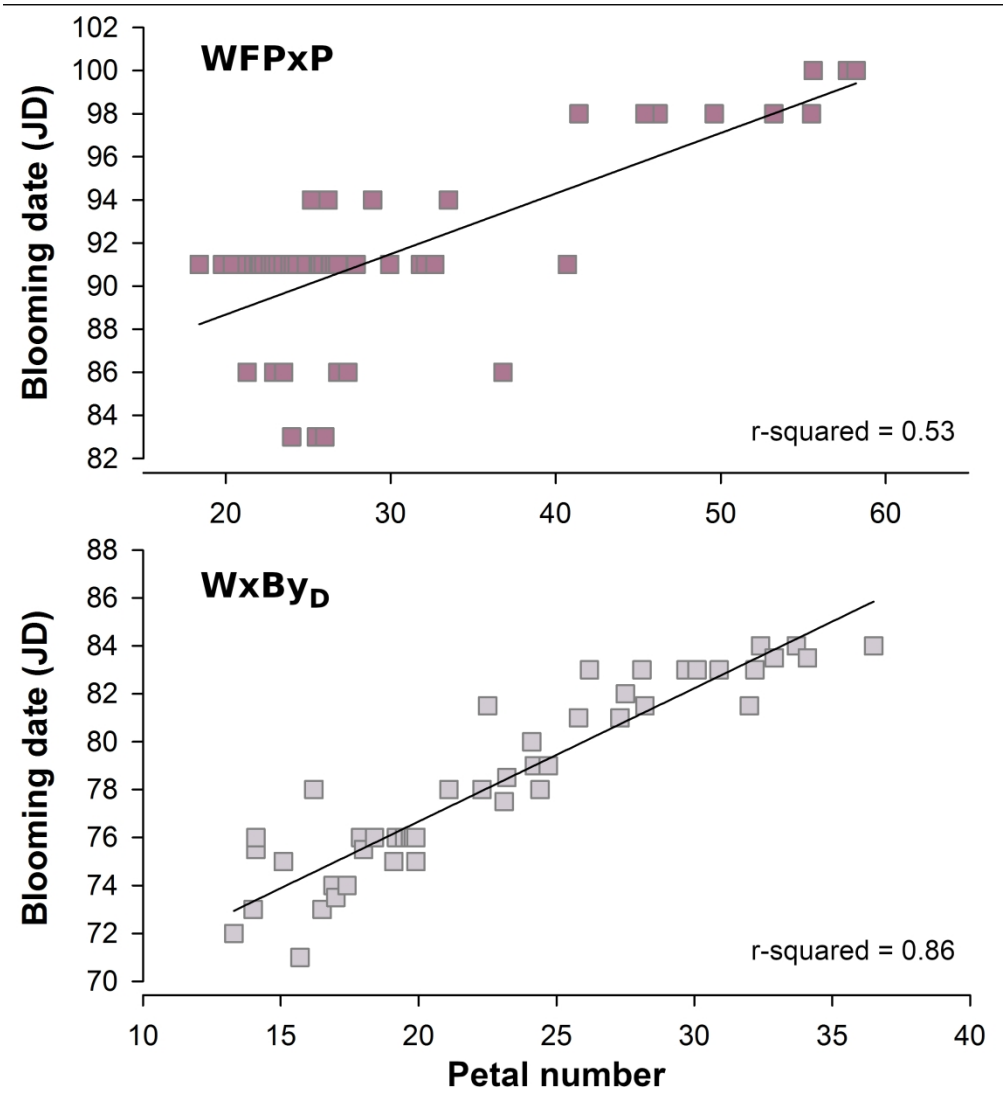
WFPxP
Blooming date (JD)
r-squared = 0.53
WxBy$_D$
Blooming date (JD)
r-squared = 0.86
Petal number

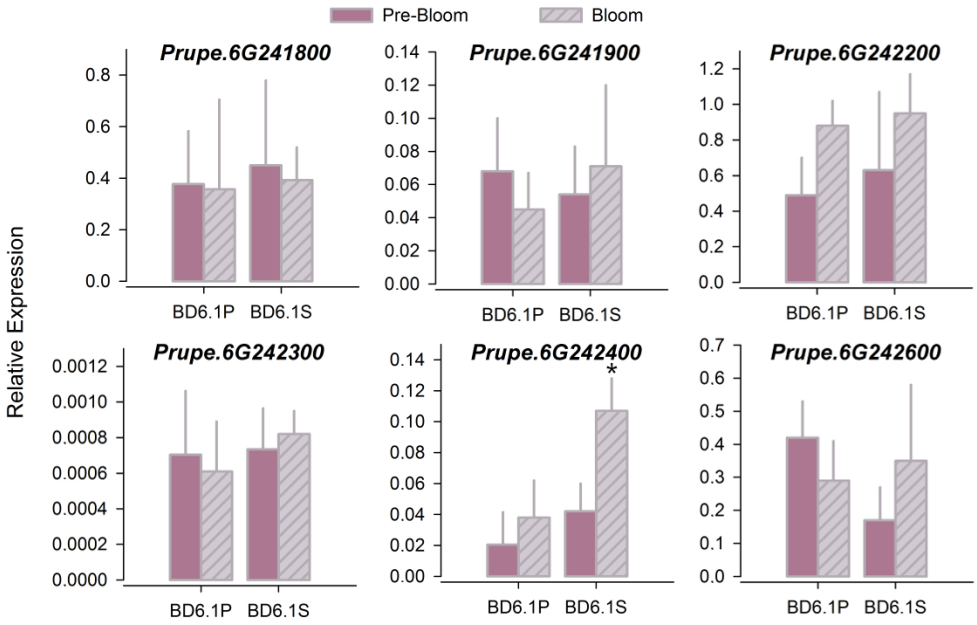
Pre-Bloom
Bloom
Relative Expression
Prupe.6G241800
Prupe.6G241900
Prupe.6G242200
Prupe.6G242300
Prupe.6G242400
Prupe.6G242600
*
BD6.1P
BD6.1S

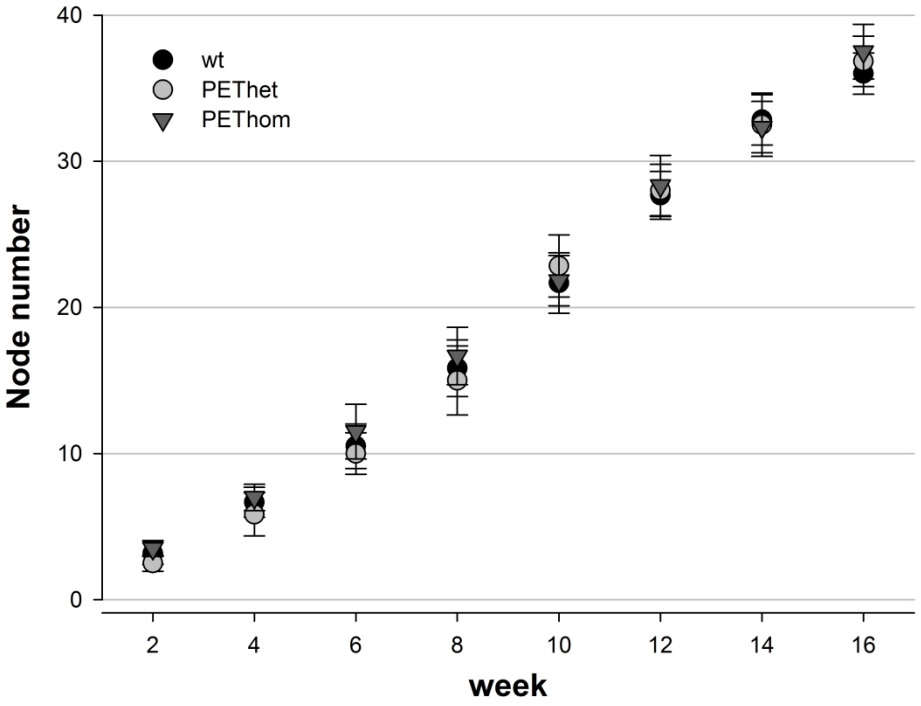
wt
PEThet
PEThom
Node number
week
0
10
20
30
40
2
4
6
8
10
12
14
16

Supplemental Table 1. List of accessions used in this study. Blooming date (BD) was recorded during seasons 2012 and 2013 and expressed in Julian Days (JD). Double-flower accessions are underlined.

Accession	Blooming Date (JD)		Accession	Blooming Date (JD)		Accession	Blooming Date (JD)	
	2012	2013		2012	2013		2012	2013
391C12XXXIV86	82	99	FFF7910001		103	RASCIADENTE GIALLA	85	
A15	82	-	FIRERED	85	101	REBUS 028	81	98
A219	81	98	FORLI1	86	103	REBUS 038	85	101
AFRA T	84	103	GG30	84	99	REBUS 195	83	101
ALBATROS	83	99	GLOHAVEN	85		REGINA D OTTOBRE	88	104
ALEXA	82	100	GOLDCREST	80	99	RICH LADY	84	102
ALIBLANCA	84	102	HARDIRED	84	101	RISING STAR		102
ALICECOL	86	103	HARROW BLOOD		98	ROMAGNA 3000	84	102
ALIPERSIE	83	101	HELENA CLING		100	ROMAGNA BIG	83	102
ALMA	83	101	IFF691	85	103	ROMAGNA BRIGHT	83	101
ANGELO MARZOCCHELLA	82	100	IFF331	87	106	ROMAGNA QUEEN	82	101
ANTONY	82	101	IONIA	89	105	ROMAGNA RED	81	100
AURORA	80	-	ISKRA	82	100	ROMAMER	80	98
AUTUMN GRAND	80	98	J. H. HALE	82	100	ROSA DARDI	88	103
AZURINA	85	102	JING YU	89		ROSELLA		100
AZURITE	85	102	JUNE PRINCESS	80	97	ROYAL ESTATE		102
BELLA CONTADINA	81	101	KAMARAT	85	103	ROYAL JIM		99
BELLA DI BORGO D'ALE	84	103	KAWEAH	86	103	ROYAL GLORY	82	
BELLA DI CESENA	84	101	KEVINA	81	99	ROYAL LEE	85	
BELLA DI PIANGIPANE	83	102	KV930455	82	100	RUBIETTE	84	98
BIG BANG	82	100	LUCREZIA	81	100	S5898:128		102
BIG TOP	80	100	LUSA	85	102	S6699	82	101
BLUSHING STAR	-	102	MARLI	81	98	SAN GIORGIO	85	
BO96025035	-	102	MARUJA	83	102	SENTRY	84	
BO92050005	**91**	**108**	MAY GRAND	84	98	SIBERIAN C	86	102
BO92050007	**90**	**108**	MAYCREST	80	99	SOUTHERN PEARL		98
BO99018028	**91**	**108**	MAYFIRE	80	99	SPLENDOR	83	101
BORDO	82	99	MERRIL GEM FREE	82	102	SPRING BABY		101
BORGIA	81	98	NADIA		101	STARK RED GOLD	82	100
BOTTO	86		NECTAGRAND	83	101	STONEY HARD	90	107
BOUNTY	82	101	NJ307	90	105	SUPEACH FOUR		101
BUCO INCAVATO I	-	103	**NJ WEEPING**	**89**	**108**	SUPEACH SIX		99
CAPUCCI 18	-	101	NJC113	81	99	SUMMER RICH	83	
CHIMARRITA	83	97	OURO IAPAR	80	101	S. MELODY x W. GLORY	82	102
CINZIA	85	101	P1-5	81	98	TARDIGOLD	83	100
CLAUDIA	87	103	P2152N	83	104	TARDIVA SPADONI	82	100
D4162	88	105	PAOLA CAVICCHI	84		VALERIA	89	106
DIXIRED	88	-	PERCOCA BIANCA MAZZINI	87	101	VISTA RICH	84	102
DOFI88338026	82	101	PESCA SETTEMBRINA	83	101	VITTORIO EMANUELE		106
DOLORES	82	101	PIERI81	83	100	XIA HUI	82	102
EARLY TOP	80	97	PLOV52N	85	103	ZAO XIA LU		102
EARLY ZEE	-	101	PPER11N	87	104	ZEE DIAMOND	80	97
ELBERTITA	83	99	PPRL11N	85	103	ZEE LADY	84	101
ELEGANT LADY	81	98	PVIN1N	88	104			
FEI CHENG BAI LI	85	-	RASCIADENTE BIANCA	85	103			

Supplemental Table 2. List of primers used in this study.

Primer name	Sequence
Fine-mapping	
BD686For	GAATTAAGGAGCGAGCAATTAT
BD686Rev	GCAACAAACTAATATTAATTCA
BD097For	CTACTTTCTAACTGGATTCTTT
BD097Rev	CAGTATTAAGTTAATTGTTTGAT
BD798_For	GAGGACCAAGACATCGATCCAGT
BD798_Rev	TCTTCTGACTCGACTTCTTCCAG
BD609_For	GACATTGTTTTAAGTCTAAGGA
BD609_Rev	CTTCTTTCTAACCTTCTCCTTT
qPCR	
Prupe.6G241800For	CCAGAGAGAGAAGAGGAAGACAAT
Prupe.6G241800Rev	CCCTCCATCTCTCTGTATCTAGTG
Prupe.6G241900For	TGCCTTCTTCTTTAACGAACCTAC
Prupe.6G241900Rev	ACCACTTTATTGAGAAGACCCAAC
Prupe.6G242000For	ATTTCCAGTGCTTTCCTCATCAAT
Prupe.6G242000Rev	CTTCCCATAATCAACCATCAGCTT
Prupe.6G242100For	CAGTTTCAAAGACAAATGACCGAC
Prupe.6G242100Rev	ATGTAATGTGGAAATTGAGGGGAG
Prupe.6G242200For	GGAGTTGTTGCTGTGGAAATTACA
Prupe.6G242200Rev	ACCAAAGACATCCCTCAAATGATC
Prupe.6G242300For	CTGTGAATCATTTGTTGCAACCAT
Prupe.6G242300Rev	CCAATATTCCTTCACCAACTTCCA
Prupe.6G242400For	GTTTCTGAGCTCCAAAAGAACAAC
Prupe.6G242400Rev	CACAGTTCTCATTCCTTGTTCTCA
Prupe.6G242500For	TCATGAGAGACCAAATTCCAAGAC
Prupe.6G242500Rev	AGGGAATGAGAAAGCAATGAGAAG
Prupe.6G242600For	TACGGGTCATTTGATAAGGTTTCG
Prupe.6G242600Rev	CCTAACCACTGACTGAACTTCATC
Tobacco	
BENa,b allele-specific	

NtBENa_For	TCCAGTTTTCTTATCTGATGGA
NtBENb_For	TTATCTGATATTGATAGGAG
BENa,b reverse	
NtBEN_Rev	GCCTCATTCCTAAGAAAACTAG
HRM edited site	
NtBEN_HRM_For	ACATCCTTATGGTGGGAGTCCTTC
NtBEN_HRM_Rev	GAGCAGCAGCTGAGGTTGAATTAG